RSC Advances

PAPER

View Article Online
View Journal | View Issue

Cite this: *RSC Adv.*, 2015, **5**, 93252

New hybrid materials based on halogenated metalloporphyrins for enhanced visible light photocatalysis

Janusz M. Dąbrowski,*[a] Barbara Pucelik,[a] Mariette M. Pereira,[b] Luis G. Arnaut,[b] Wojciech Macyk[a] and Grażyna Stochel[a]

Received 24th September 2015
Accepted 27th October 2015

DOI: 10.1039/c5ra19742b

www.rsc.org/advances

Photophysical and photochemical studies on 5,10,15,20-tetrakis(2,6-difluoro-5-*N*-methylsulfamylophenyl) porphyrin (F_2PMet) and its cobalt(III) and zinc(II) complexes, including spectroscopic characteristics, photostability and photocatalytic activity, were carried out. The hybrid materials resulting from adsorption of these tetrapyrroles at the surface of titanium dioxide were prepared and examined in terms of their morphological, optical and functional properties applying absorption spectroscopy, scanning electron microscopy (SEM), photoelectrochemistry and photocatalytic tests. Our studies revealed that MF_2PMet@TiO_2 photocatalysts can be considered as the hybrid organic/inorganic photoactive materials enabling photodegradation of a synthetic opioid such as tramadol hydrochloride (TRML) and a model pollutant, 4-chlorophenol, in aqueous solution under visible light irradiation ($\lambda > 400$ nm). To elucidate mechanisms of photochemical processes, the photocatalytic activity of investigated metalloporphyrins was compared in homo- and heterogeneous systems. The results indicate that impregnation of TiO_2 (P25) with functionalized porphyrins can improve its photoactivity. ZnF_2PMet@TiO_2 exhibited a superior photocatalytic performance towards TRML degradation. The role of singlet oxygen and hydroxyl radicals in photodegradation processes has been elucidated both for MF_2PMet and MF_2PMet@TiO_2 systems.

1. Introduction

The importance of reactive oxygen species (ROS) production in biological and environmental processes is very well established. Among ROS, singlet oxygen[1] ($^1O_2$) is a particularly interesting photogenerated oxidant since it plays a key role in several processes, such as photodynamic therapy of cancer,[2–5] inactivation of microorganisms,[6] oxidative stress[7] and photodegradation of dyes, polymers or other organic compounds.[8,9] Nowadays the development of novel photomaterials for efficient generation of singlet oxygen is of great interest. Porphyrins have been recently shown to be effective generators of ROS.[10–12] The permanent popularity of these tetrapyrrolic compounds is determined by their efficient absorption of visible light, high quantum yield of triplet state formation and consequently long triplet state lifetimes.[13,14] Moreover, they play critical roles in many biological processes. The studies on their photophysical properties have been extended to important and hot topics, such as dye-sensitized solar cells,[15] optoelectronics,[16] photomedicine[17,18] and photocatalysis.[19] In the case of porphyrins and other tetrapyrrolic photosensitizers, coordination of a metal ion seems to be an obvious way to change the properties of both the ground and excited states.[20] Metalation not only modulates spectroscopic and photophysical properties of these photosensitizers, but also modifies their hydrophobicity, stability, degree of aggregation and, consequently, the efficacy in photooxidation processes.[21] There are serious environmental concerns on the levels of organic dyes in waste and groundwater. Among several methods, photooxidation is probably the most promising and low-cost methodology to achieve the degradation of these pollutants in environment employing solar light, oxygen and a photocatalyst (sensitizer).[22–24] Although a significant progress has been achieved in the field of photocatalysis, the development of novel efficient photocatalysts and investigation of various approaches to improve the performance of semiconductor-based photocatalytic redox processes remain very active research fields.[25–27]

For tests of photocatalytic degradation of pollutants several model pollutants can be applied. In this paper we describe the photoactivity of sensitizers in the oxidation of 4-chlorophenol (4-CP) and tramadol hydrochloride (TRML). 4-CP is a model molecule for the oxidization by hydroxyl radicals. TRML is a synthetic opioid aminocyclohexanol type drug that can pollute water, and very little is known about its elimination and photodegradation in environment.[28] It was recently shown that tramadol is very poorly degraded, both biologically and photochemically, in aqueous environments. For instance, a decrease by only 25% of TRML initial concentration ($c_0 = 10$ mg L^{-1}) was

[a]*Faculty of Chemistry, Jagiellonian University, Ingardena 3, 31-060 Kraków, Poland. E-mail: jdabrows@chemia.uj.edu.pl; Fax: +48 126340515; Tel: +48 126632293*
[b]*Chemistry Departament, University of Coimbra, Rua Larga, Coimbra, Portugal*

observed after 128 min of irradiation with the Xe lamp.[29] UV-induced HO$^{\bullet}$ appears to play a significant role in this degradation process. However, other ROS such as singlet oxygen, superoxide ion and hydrogen peroxide, are also suggested as potential oxidants.[30]

Recently, we have shown that 5,10,15,20-tetrakis(2,6-dichloro-3-sulfophenyl)porphyrin and some of its metal complexes are efficient sensitizers for the degradation of phenols, chlorophenols and atrazines in water.[31] Moreover, we have demonstrated that sulfonated and sulfonamide dihydro- and tetrahydroporphyrins with halogen atoms in the *ortho* positions of the phenyl rings have shown very high phototoxicities towards various cancer cells *in vitro*[3,32] and tumors *in vivo*,[33] and that their efficacy is much higher than that of the other sensitizers.[13] Some of the photophysical properties of F_2PMet and ZnF_2PMet have been previously studied. The singlet oxygen quantum yield (Φ_Δ) and *in vitro* activity against human lung adenocarcinoma cell line (A549) were evaluated and shown that that the efficacy of photodynamic therapy strongly depends on the nature of ROS generated during irradiation.[34] The coordination of porphyrins with metal ions (*e.g.* Zn^{2+}) has been frequently used to stabilize the porphyrin ring, while maintaining most of the photophysical properties necessary for PDT and also for photocatalysis.[35,36] By studying the photophysical properties relevant to photocatalysis within a series of materials we expect to show how modification of macrocycle *via* metal insertion and functionalization of TiO_2 surface with various metal complexes of halogenated porphyrin can affect ROS generation and photocatalytic activities in both homogeneous and heterogeneous systems.

In this paper we describe the spectroscopic and photochemical properties of *meso*-tetrakis(2,6-difluoro-5-*N*-methylsulfamylophenyl)porphyrin and the corresponding, cobalt(III) and zinc(II) complexes, presented in Chart 1. Additionally, we prepared TiO_2-based materials impregnated with selected (metallo)porphyrins and extended these studies to the photodegradation of organic model pollutants (TRML, 4-CP) using the new compounds and visible light. We also performed photoelectrochemical measurements, adsorption isotherms to elucidate details of mechanisms of the photophysical and photochemical processes and detection of ROS.

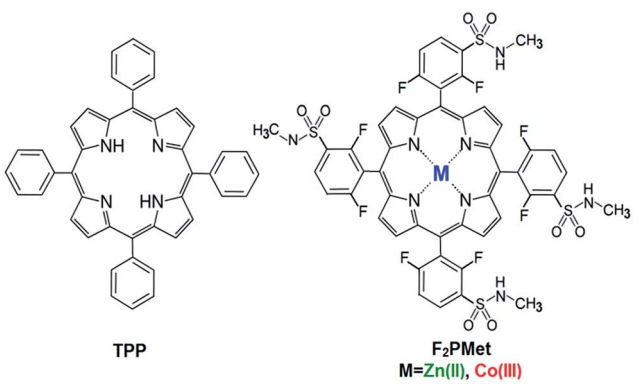

Chart 1 Chemical structures of *meso*-tetraphenylporphyrin (TPP) and metal (M) complexes of *meso*-tetrakis(2,6-difluoro-5-*N*-methylsulfamylophenyl)porphyrin (F_2PMet).

2. Experimental methods

2.1. Chemicals

All chemicals were of a reagent grade and used as received. Solvents used in the synthesis of the photosensitizers were purified and dried using standard methods. The chloroform used in the preparative thin layer chromatography was neutralized with neutral active alumina. Solutions were prepared with doubly distilled water, either equilibrated with air or bubbled with argon at room temperature. Reactions were carried out under a nitrogen atmosphere and were monitored by TLC (0.20 mm analytical silica plates).

2.2. UV/VIS absorption spectra and photodegradation experiments

UV/VIS absorption spectra were recorded in quartz cuvettes with Shimadzu 2100 or Hewlett Packard HP8453 spectrophotometers. In order to check photostability of the sensitizer, irradiation of the solution was carried out using the xenon lamp (XBO-150) through the 10 cm water filter and 320 nm or 420 nm cut-off filters delivering *ca.* 75 mW cm^{-2}, as measured at the surface of the cuvette. Solutions containing samples of photosensitizers were dissolved in ethanol or water and irradiated in quartz cuvettes. The absorption spectra were recorded before and immediately after irradiation within 5 and 60 minutes.

2.3. Photocatalytic activity of halogenated metalloporphyrins in homogeneous systems

Photocatalytic activity was tested by monitoring the progress of tramadol hydrochloride and 4-chlorophenol (both purchased from Sigma-Aldrich) photodegradation in ethanol/water solutions (1 : 99 v/v). Continuous irradiation of an aerated solution of sensitizers and model pollutants (*ca.* 5×10^{-5} M) were carried out using the xenon lamp (XBO-150) through the 10 cm water filter and bandpass filter transmitting within 330–500 nm range, delivering 75 mW cm^{-2}. Application of this filter enabled excitation of metalloporphyrins within their Soret band with excitation of neither 4-CP nor TRML. The reaction progress was monitored by UV/VIS spectroscopy using a Hewlett Packard HP8453 spectrophotometer.

2.4. Porphyrins@TiO_2 materials preparation

Photocatalysts were prepared by suspending the *ca.* 0.1 g Degussa P25 TiO_2 powder (composed of anatase 70% and rutile 30%) with ethanol/water (1 : 99 v/v) solution of selected (metallo)porphyrins (5 mL, 5×10^{-5} M). The mixtures were stirred, and samples were filtered and washed several times with water in order to remove the unadsorbed porphyrin. TiO_2 impregnated with MF_2PMet (abbreviated as MF_2PMet@TiO_2, M = Zn(II), Co(III)) was obtained after centrifugation and dried in oven (at *ca.* 60 °C) overnight.

2.5. Diffuse reflectance measurements

Diffuse reflectance spectra were recorded with a Shimadzu 3600 UV-VIS-NIR spectrometer equipped with a 6 cm dia. integrating

sphere. Prior to the measurements the samples were ground in the agate mortar with barium sulfate (*ca.* 1 : 50 wt ratio) and placed in round holder to form a pellet (diameter *ca.* 2 cm). The reflectance of prepared materials was recorded using $BaSO_4$ as a reference.

2.6. Adsorption isotherm measurements

To test the surface coverage, 0.1 g TiO_2 (P25) was suspended in 5 mL of ethanol : water solution (1 : 99) of each porphyrin (5–500 μM). A second set of solutions with the same concentrations of porphyrin, but without TiO_2, were also prepared. The suspensions with TiO_2 were mixed and stored in the dark overnight at RT. After centrifugation the concentration of porphyrin in supernatant solution was determined spectroscopically by measuring the absorbance at Soret band. Moreover, for prepared and dried (60 °C, 12 h) materials diffuse reflectance spectra were measured. The difference in absorbance between the solutions with and without porphyrin and the changes in diffuse reflectance spectra were used to determine the equilibrium concentration of the solution and the amount of porphyrin adsorbed at TiO_2.

2.7. Characterization of $MF_2PMet@TiO_2$ materials using scanning electron microscopy (SEM)

The morphologies of unmodified TiO_2 and modified TiO_2-based materials: $F_2PMet@TiO_2$, $CoF_2PMet@TiO_2$ and $ZnF_2PMet@TiO_2$ were examined by scanning electron microscope (Vega 3 LM, Tescan, equipped with the LaB_6 cathode, operated at a voltage of 30 kV).

2.8. Photolectrochemical measurements

A three-electrode set-up was used for electrochemical measurements. The electrolyte (0.1 M tetrabutylammonium perchlorate, TBAP, in ethanol) solution was air-equilibrated. Platinum and Ag/AgCl were used as counter and reference electrodes, respectively. The electrochemical measurements (CV, photocurrent action spectra) were controlled with a BAS 50 W (Bioanalytical Systems) electrochemical analyzer. Cyclic voltammograms were recorded at a scan rate of 10 mV s^{-1}. Photocurrent action spectra were recorded under potentiostatic conditions at 700 mV *vs.* Ag/AgCl, and were not corrected for changes in light intensity.

2.9. Photocatalytic activity of TiO_2-based hybrid materials functionalized with halogenated metalloporphyrins

The photocatalytic activity of modified-TiO_2 materials was estimated by measuring the decomposition rate of 4-CP and TRML in an aqueous solution. The samples (10 mg, 20 mL) of TiO_2 impregnated with metalloporphyrins in solution of model pollutants (2.5×10^{-4} M) were stirred and irradiated in a cylindrical quartz cuvette using the xenon lamp (XBO-150) through the water filter and the 400 nm cut-off filter. Before the analysis samples were collected and filtered through the Millipore membrane filter. The absorption spectra during experiments were recorded after irradiation times between 10 and 60 minutes and the degradation of 4-CP and TRML was monitored at 280 nm and 271 nm, respectively. Absorption spectra were collected at Hewlett Packard HP8453 spectrophotometer. To test the role of various reactive oxygen species (hydroxyl radicals or singlet oxygen) a solution of photocatalysts and TRML was irradiated in the presence of selected ROS scavengers: sodium azide (NaN_3) and sodium ascorbate (Asc) at 1×10^{-2} M concentration. In addition, the oxidation of terephthalic acid (TA) was carried out according to the following procedure: photocatalyst – $ZnF_2PMet@TiO_2$ was added to TA aqueous solution (6×10^{-3} M TA, 0.02 M NaOH) and the suspension was irradiated for 60 min. Sample aliquots were collected during reaction, which were then filtered and quantified by measuring the formation of the hydroxyterephthalic acid (TAOH) by fluorescence spectroscopy at $\lambda_{exc} = 312$ nm, $\lambda_{em} = 350$–500 nm ($\lambda_{max} = 425$ nm) using LS Fluorescence Spectrophotometer (Perkin-Elmer). Moreover, photocatalytic efficacy of $ZnF_2PMet@TiO_2$ was compared to that of unmodified TiO_2 (P25) in an analogous experiment.

3. Results and discussion

3.1. Photosensitizers

Meso-Tetrakis(2,6-difluoro-5-*N*-methylsulfamylophenyl)porphyrin (F_2PMet) was synthesized according to a previously described method.[37,38] Its chemical structure together with the structure of tetraphenylporphyrin (TPP) are presented in Chart 1. In brief, the halogenated tetraphenylporphyrin was prepared by condensation of pyrrole with 2,6-difluorobenzaldehyde using acetic acid/nitrobenzene as a solvent.[12] Chlorosulfonation reaction of the halogenated tetraphenylporphyrin, followed by a nucleophilic substitution with amines, gave the amphiphilic sulfonamide halogenated porphyrin. Metalation of this porphyrin was achieved by refluxing it with the appropriate metal sulphate in *N*,*N*-dimethylformamide. The reaction was monitored by UV/VIS absorption spectroscopy and was stopped when the characteristic four Q bands of free porphyrin disappeared and the spectrum of metalloporphyrin evolved. The final step consisted of the hydrolysis of the chlorosulfonated metalloporphyrin (80 mg, 120 mL of water) for 20 hours to give the corresponding sulfonamide metalloporphyrin.

3.2. Spectroscopic characterization of photosensitizers

The ground state absorption spectra of F_2PMet and its Zn(II) and Co(III) complexes recorded at room temperature in ethanol are presented in Fig. 1. The spectrum of F_2PMet shows the characteristic bands originated from free base porphyrin with the D_{2h} symmetry, described by a four orbitals model. The intense Soret band is observed at 410 nm, Q_x, Q_y and two additional bands are observed at 505, 537, 582 and 639 nm. These extra bands are due to vibrational coupling effects and originate from HOMO (b_{1u} orbital) to the first vibrationally excited state of LUMO (b_{2g} orbital) or to LUMO+1 (b_{3g} orbital) transitions.[13] The insertion of Zn^{2+} to the free base porphyrin leads to a significant red shift of the Soret band (410 → 420 nm) and the replacement of four Q bands into two bands at 549 and 588 nm.

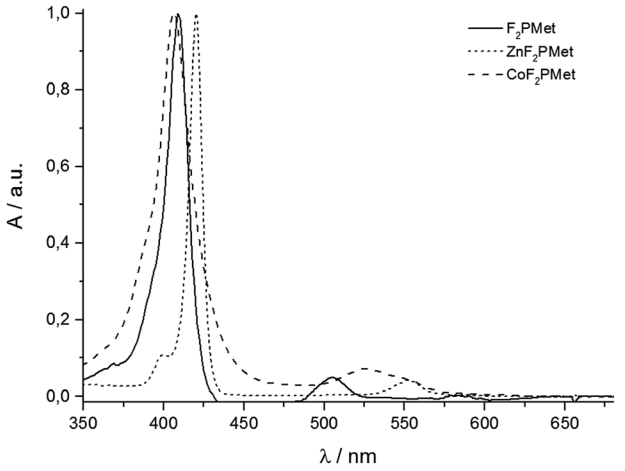

Fig. 1 Electronic absorption spectra of F_2PMet, ZnF_2PMet and CoF_2PMet measured in ethanol at room temperature.

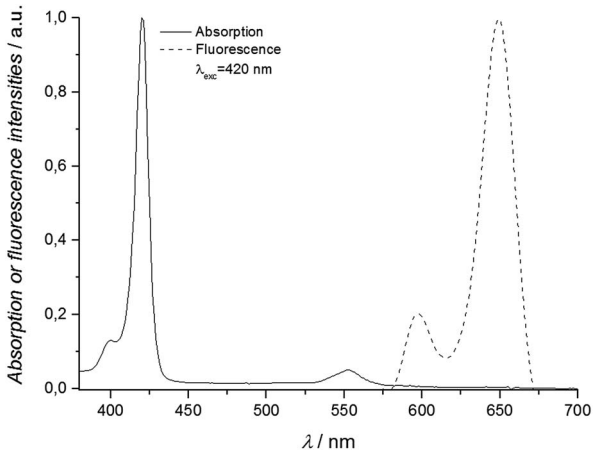

Fig. 2 Electronic absorption and fluorescence spectra of ZnF_2PMet measured in ethanol at room temperature.

In addition, a slight hipsochromic shift of the Soret band is observed for CoF_2PMet (410 → 408 nm). The number of Q bands always decreases upon the coordination of the metal ions to free base porphyrins because of the change of symmetry, from D_{2h} to D_{4h}. According to Gouterman's four-orbitals model, formation of metalloporphyrins enforces the degeneracy of the two molecular orbitals: LUMO and LUMO−1 and the absorption spectra show only two Q bands. The fourfold rotational symmetry of ZnF_2PMet is also reflected in the coincidence of the *x*- and *y*-components of the Q bands (Q_{xy}) and may result in enhancement of the molar absorption coefficient values, while the lower symmetry of the free base porphyrin is indicated by the splitting of the Q bands into Q_x and Q_y. Because of the interaction between the central zinc ion and the π-conjugate system, the Q bands of the zinc porphyrin are characterized by higher values of molar absorption coefficients than the metal-free and cobalt(III) complexes. The electronic absorption and fluorescence spectra of the representative metalloporphyrin (ZnF_2PMet) are shown in Fig. 2. The fluorescence quantum yield determined for F_2PMet is reduced by a factor of two. This is consistent with the internal heavy atom effect discussed below. A further decrease of Φ_F is observed for ZnF_2PMet ($\Phi_F = 0.001$). Metalloporphyrins with closed metal shells are less fluorescent than the corresponding free bases. Moreover, they have higher efficiencies of intersystem crossing to the triplet state promoted by the spin–orbit coupling mechanism. Paramagnetic complexes, such as CoF_2PMet, have one odd electron that can couple to the spin of the porphyrin triplet yielding "tripdoublet" and "tripquartet" states. Similarly, that odd electron can couple its spin with that of the porphyrin first excited singlet state, leading to singmultiplet states. The singmultiplet states couple efficiently with the tripmultiplet states resulting in a rapid intersystem crossing from the excited singlet state to the triplet state.[13] This coupling mechanism deactivates the singlet states rapidly and quenches almost completely the fluorescence of paramagnetic complexes of porphyrins ($\Phi_F \leq 7 \times 10^{-5}$). The fluorescence excitation spectra of all fluorescent compounds correspond well with their absorption spectra and confirm the purity and non-aggregation of the samples.

Earlier studies with other halogenated porphyrins revealed that the presence of chloro-groups in *ortho* positions reduced the tendency of porphyrins to aggregate.[12] The fluorescence quantum yields of these porphyrins were also determined according to the published procedures[4] using TPP as a reference ($\Phi_F = 0.11$). All determined spectral parameters are given in Table 1. In our previous work the quantum yield of singlet oxygen formation was also evaluated and reached 0.71 for F_2PMet and 0.99 for ZnF_2PMet, indicating that these porphyrins in solution are efficient singlet oxygen generators.[34] These data also suggest that the increase in Φ_Δ is related to an increase of the triplet state quantum yield. The internal heavy atom effect assists halogenated porphyrins to generate triplet states with quantum yields approaching a unity. The introduction of Zn^{2+} into tetraphenylporphyrin derivatives improves photochemical properties influencing photodynamic and photocatalytic activity.

3.3. Photodegradation in homogenous system

In the presence of visible light and oxygen porphyrins in aqueous solutions undergo a decomposition reaction. Thus, the stability of metal complexes with halogenated sulfonamide porphyrin has to be estimated under experimental conditions. Photobleaching experiments revealed a good stability of metalloporphyrins under xenon lamp irradiation (Fig. 3a and b).

The improved stability compared to TPPS results from the introduction of electron-withdrawing fluorine atoms in the *ortho* positions of the phenyl rings. The studied compounds have also sulfonamide substituents in the *meta* positions of the phenyl rings which additionally stabilize the porphyrin structure. The fastest photobleaching of CoF_2PMet in water can be attributed to the photo-Fenton-like reactions leading to the generation of hydroxyl radicals.[39,40] In addition to the generation of ROS by Co(II), it has been shown that the Fenton-like reaction mixture containing even small amount of cobalt(II) had strong pro-oxidative effects.[41] This hypothesis is further

Table 1 Spectroscopic properties of fluorinated porphyrin (F_2PMet), its metal complexes and the reference (TPP) determined in ethanol

	Absorption					Fluorescence	
	λ (nm), ε (M^{-1} cm^{-1}) $\times$ 10^3					λ (nm)	
	B	Q_y (0-1)	Q_y (0-0)	Q_x (0-1)	Q_x (0-0)	(0-0) (1-0)	Φ_F
TPP	**417**, 16.0	**549**, 7.00	**513**, 1.20	**590**, 2.50	**649**, 0.50	650;711	0.09
F_2PMet	**410**, 379	**537**, —	**505**, 25	**582**, 7.70	**639**, **0.70**	650;731	0.05

	Absorption			Fluorescence	
	λ (nm), ε (M^{-1} cm^{-1}) $\times$ 10^3			λ (nm)	
	B	Q_{xy} (0-1)	Q_{xy} (1-0)	(0-0) (1-0)	Φ_F
ZnF_2PMet	**420**, 496	**588**, 16.8	**549**, 14.8	599;651	0.001
CoF_2PMet	**408**, 367	**569**, 3.1	**530**, 18.0	599;651	5×10^{-5}

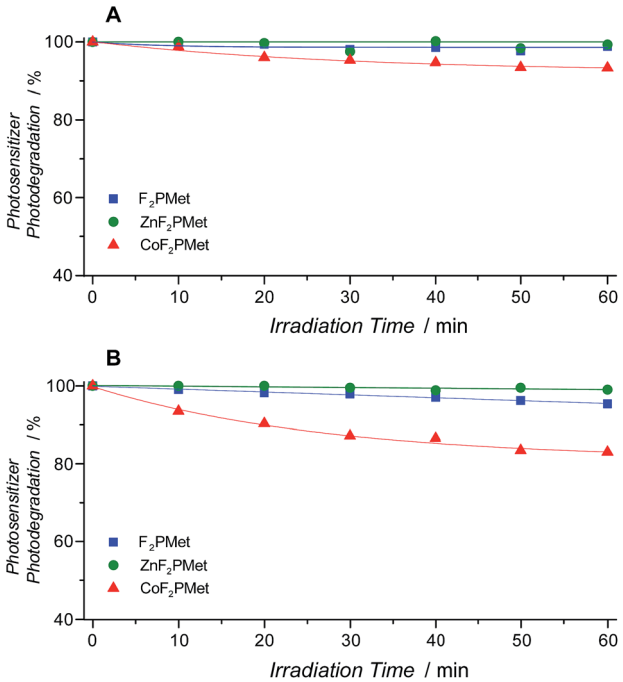

Fig. 3 Photostability of sulfonamide halogenated porphyrin and its metal complexes in ethanol (a) and water (b) solutions. Irradiation of the solutions was carried out using 75 W xenon lamp through water filter and 320 or 420 nm cut-off filters.

supported by an improved stability of the complex in ethanol (compared to an aqueous solution), which efficiently scavenges HO$^{\bullet}$, but increases lifetime of $^1O_2$.

3.4. Photocatalytic degradation of 4-chlorophenol and tramadol hydrochloride in homogeneous system

Photodegradation tests of model pollutants were performed to assess the influence of central metal ion in the photocatalytic efficiency in homogeneous system. 4-Chlorophenol and tramadol hydrochloride (Chart 2) were selected for these photocatalytic studies.

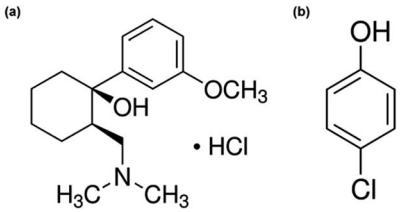

Chart 2 Chemical structures of tramadol hydrochloride (a) and 4-chlorophenol (b).

Photodegradation of these model compounds in the presence of different metalloporphyrins is presented in Fig. 4. Under tested conditions neither 4-CP nor TRML underwent appreciable photodegradation in the absence of any metalloporphyrins. The lowest photocatalytic activity was observed in the case of F_2PMet, both in the experiment with 4-CP and TRML. The other two metalloporphyrins showed a comparable photoactivity in the tests of 4-CP degradation. To the best of our knowledge, no studies have been published on the efficacy of metalloporphyrins towards tramadol photodegradation. As seen in Fig. 4b degradation of TRML differentiates the photocatalysts under tested conditions, with their photoactivity following the order: F_2PMet < CoF_2PMet < ZnF_2PMet. The differences in degradation paths of 4-CP and TRML lead to some conclusions on ROS photodegradation by the metalloporphyrins investigated in this work. ZnF_2PMet produces the highest amounts of singlet oxygen and is the most photostable of the homogeneous systems studied in this work. Hence, its photocatalytic activity is expected to be the highest of this family of photosensitizsers. On the other hand, the lower stability of CoF_2-PMet compared to other porphyrins, and assigned to the generation of hydroxyl radicals under tested conditions, impairs its photocatalytic activity at longer irradiation times, especially in water. Therefore for long-term irradiations ZnF_2PMet appears to be the most promising photocatalyst. The competiveness of CoF_2-PMet towards 4-CP photodegradation suggests that the limitations of this photocatalyst are somewhat compensated by its ability to participate in photo-Fenton-like reactions.

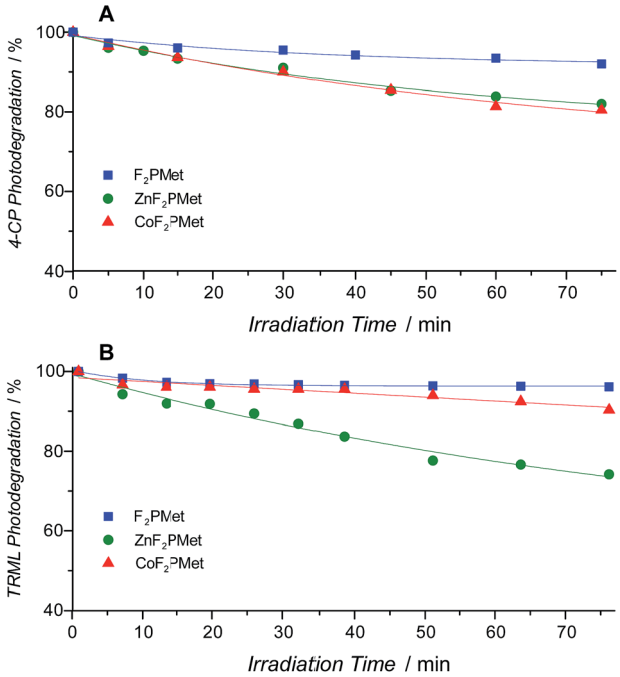

Fig. 4 Photodegradation of 4-CP (a) and TRML (b) in the presence of various photocatalysts (F_2PMet, ZnF_2PMet, CoF_2PMet) in homogeneous system upon irradiation with 75 W xenon lamp through the 400 nm cut-off filter.

3.5. Adsorption of (metallo)porphyrins on TiO_2 and their spectroscopic characteristics

Diffuse reflectance spectra of unmodified TiO_2 (P25) and surface-modified (metallo)porphyrin materials converted to the Kubelka–Munk function are presented in Fig. 5. The adsorption of the (metallo)porphyrins at the surface of TiO_2 leads to a significant red shift of the absorption bands (*ca.* 8 nm). In the control experiment in which diffuse reflectance spectra of porphyrins in the presence of $BaSO_4$ were recorded, such changes were not observed.

The RT adsorption isotherms for F_2PMet, ZnF_2PMet and CoF_2PMet are shown in Fig. 6. Above 250 μM the isotherms tend

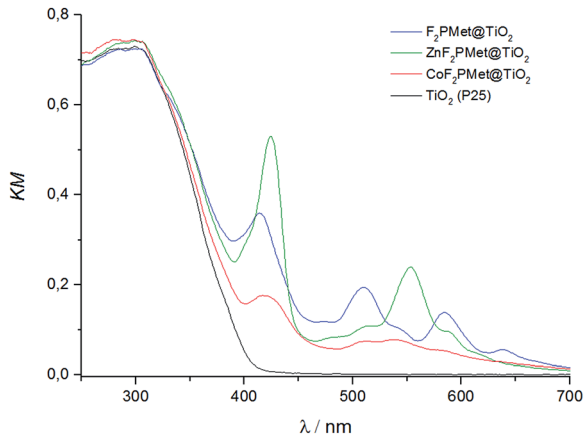

Fig. 5 Diffuse reflectance spectra of the surface modified TiO_2 (P25) materials.

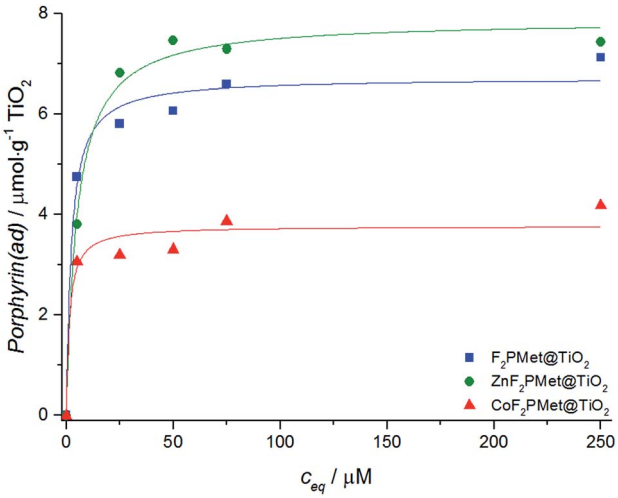

Fig. 6 Adsorption isotherm for F_2PMet, ZnF_2PMet and CoF_2PMet on TiO_2 (P25) at RT. The line shows the fit to the Langmuir model.

Table 2 Adsorption parameters of the hybrid materials

Material	Q_{sat}	K_{ad}
F_2PMet@TiO_2	6.7	0.43
ZnF_2PMet@TiO_2	7.9	0.70
CoF_2PMet@TiO_2	3.8	0.20

to curve upwards, indicating a multilayer adsorption (data not shown). The data from 0 to 250 μM were fitted to a Langmuir isotherm. The maximal coverage obtained for ZnF_2PMet was 7.9 μmol per gram of TiO_2 (P25), while for F_2PMet and CoF_2PMet the coverage reached 6.7 and 3.8 μmol g^{-1}, respectively. Adsorption parameters of all studied materials are listed in Table 2. The highest equilibrium constant for ZnF_2PMet adsorption indicates that the porphyrin is strongly chemisorbed, as expected.

3.6. Morphological properties of TiO_2-based photocatalysts

The SEM images of unmodified TiO_2 (P25) and porphyrin@TiO_2 materials are shown in Fig. 7. It can be observed that the modified materials possess a similar morphology as bare TiO_2. However, after porphyrin impregnation, TiO_2 displays the color of the porphyrin and the surface of TiO_2 contains aggregates and becomes rougher. Accordingly, this observation may indicate that the aggregation takes place during the titanium dioxide impregnation with porphyrins. In all the cases, it is possible that the porphyrin particles have been anchored to the surface of TiO_2.

3.7. Photoelectrochemical properties of TiO_2-based photocatalysts

Measurements of photocurrent generated by metalloporphyrins adsorbed at TiO_2 surface can be used to study the process of electron transfer from the excited sensitizer. TiO_2 itself gives a clear signal (electron transfer to ITO) at the excitation range of 320–370 nm (Fig. 8a). Among the studied compounds

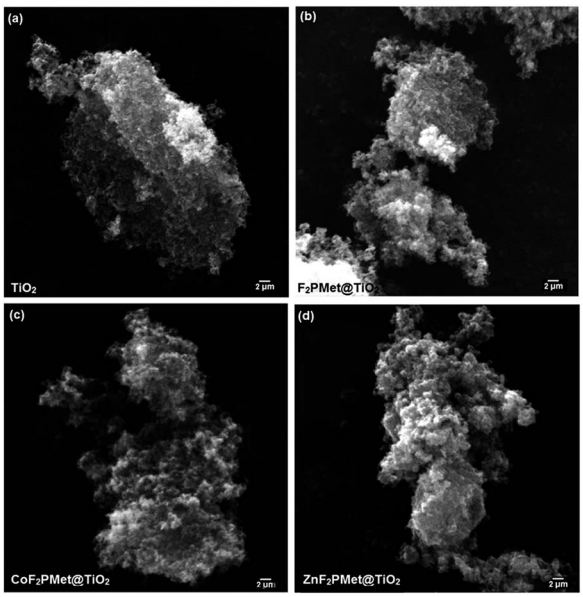

Fig. 7 SEM images of unmodified TiO_2 (a), $F_2PMet@TiO_2$ (b), CoF_2-$PMet@TiO_2$ (c), $ZnF_2PMet@TiO_2$ (d).

photocurrents above 400 nm appear for ZnF_2PMet (Fig. 8b), which are assigned to electron transfer from the excited state of porphyrin to TiO_2. ZnF_2PMet is characterized by the highest quantum yield of the triplet state formation and the longest triplet state lifetime, therefore the triplet state is very likely involved in the photoinduced electron injection from the excited state of the complex to the conduction band of TiO_2. This identifies a highly stable photocatalytic material, ZnF_2-$PMet@TiO_2$, which can promote the visible-light sensitized ($\lambda >$ 400 nm) decomposition of several representative organic pollutants.

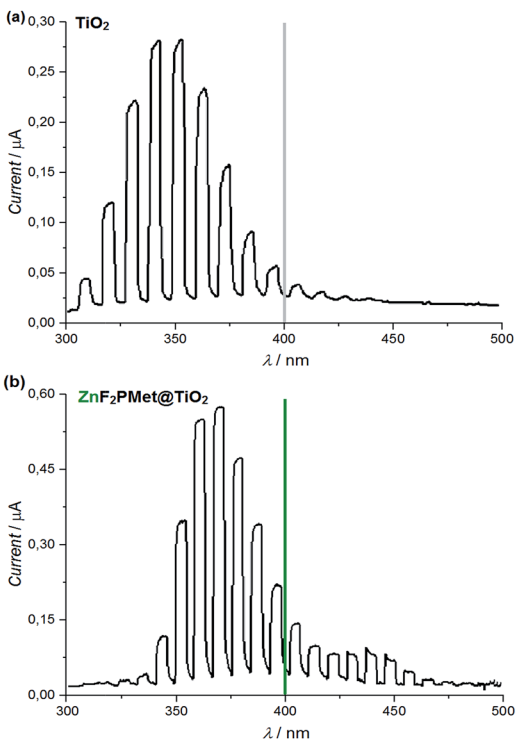

Fig. 8 Photocurrents generated at electrodes covered with TiO_2 (a) and TiO_2 with adsorbed (metallo)porphyrins (b) as a function of the wavelength of incident light (constant potentials, *ca.* 670 mV *vs.* Ag/AgCl).

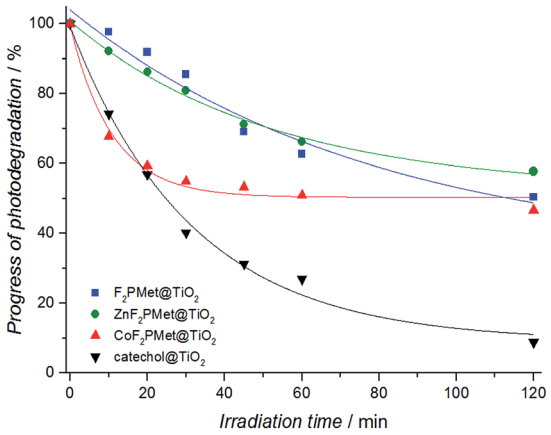

Fig. 9 Photostability of the studied materials ($F_2PMet@TiO_2$, ZnF_2-$PMet@TiO_2$, $CoF_2PMet@TiO_2$) and reference material: $catechol@TiO_2$.

3.8. Photodegradation in heterogeneous systems

In order to check the photostability of the hybrid materials, their irradiation was carried out using the xenon lamp (XBO-150). The 10 cm water filter and 400 nm cut-off filter delivering *ca.* 75 mW cm^{-2} were employed similarly to the experiments in homogeneous systems. Diffuse reflectance spectra were recorded with Shimadzu 3600 spectrophotometer using $BaSO_4$ as a reference. The spectra were recorded before and immediately after irradiation within 10–120 minutes and data were converted using Kubelka–Munk function.

For the comparison purposes, a previously studied material, $catechol@TiO_2$ [42–44] was also tested. As can be seen in Fig. 9 all newly designed materials are significantly more stable than catechol adsorbed at TiO_2. Among all photocatalysts presented in this work, $ZnF_2Pmet@TiO_2$ proved to be the most photostable one.

3.9. Photocatalytic degradation of 4-chlorophenol and tramadol hydrochloride in heterogeneous system

Recently, the photocatalytic activity of hybrid metalloporphyrin-TiO_2 materials and their versatile photocatalytic capabilities in electron transfer reaction or energy transfer under visible light irradiation have been examined on model pollutant molecules (*e.g.* methyl orange,[45] 4-nitrophenol[46]) and pharmaceuticals.[47] The photoactivity of selected synthetized metalloporphyrins adsorbed at titanium dioxide has been tested. Again, both in the case of 4-CP and TRML degradation tests the material with ZnF_2PMet showed the highest activity upon visible light irradiation (Fig. 10a and b). This result is consistent with the measurements of photocurrents, proving an efficient

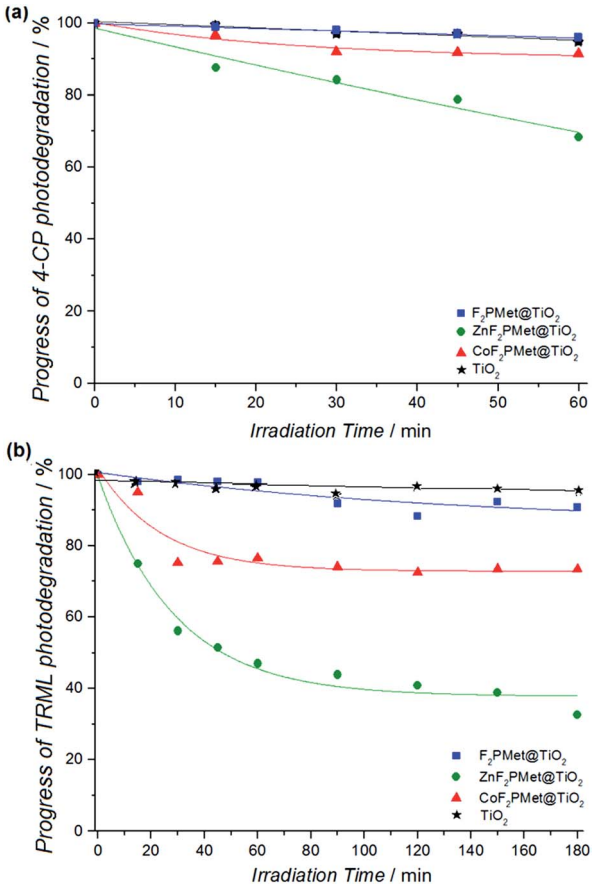

Fig. 10 Photodegradation of 4-CP (a) and TRML (b) in the presence of various TiO_2-modified materials ($F_2PMet@TiO_2$, $ZnF_2PMet@TiO_2$ and $CoF_2PMet@TiO_2$) upon irradiation through the 400 nm cut-off filter.

photosensitization of TiO_2 by ZnF_2PMet. Under visible light irradiation $ZnF_2PMet@TiO_2$ shows a high photocatalytic activity. After 1 h of irradiation it degrades 35% of 4-CP and 55% of TRML, whereas under the same conditions photodegradation of these pollutants mediated by bare TiO_2 is negligible. Visible light excites the photosensitizer and promotes the electron transfer from the macrocycle to the conduction band of TiO_2. The pollutant acts as an electron donor to regenerate the surface bound sensitizer, eliminating the need for any additional sacrificial electron donors.[48] The reaction of 4-CP and TRML decomposition involves oxidation with reactive oxygen species, in particular with hydroxyl radicals generated in consecutive reduction of oxygen to superoxide, hydrogen peroxide and finally to OH^- and $HO^\bullet$ by electrons from the conduction band. Taking into account the uncommon stability of the $ZnF_2PMet@TiO_2$ system, the material may appear a useful photocatalyst operating upon visible light irradiation. In addition, a solution of the photocatalyst and TRML was irradiated in the presence of selected reactive oxygen species scavengers: sodium azide (NaN_3) and sodium ascorbate (Asc). Their effect on the photodegradation of TRML was presented in Fig. 11. It can be observed, that when NaN_3 (a scavenger of $^1O_2$) was added, an initial acceleration followed by an inhibition of

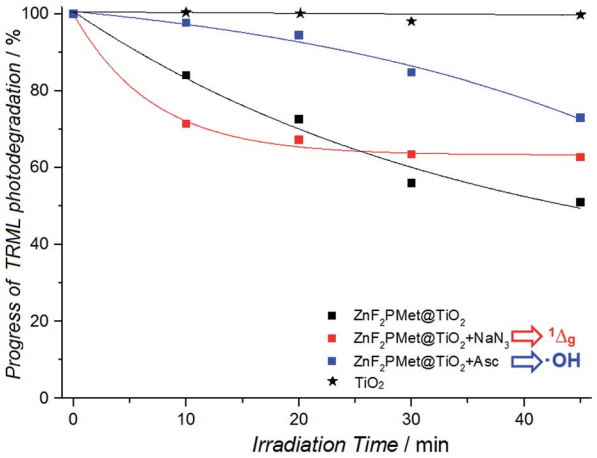

Fig. 11 Photodegradation of TRML in the presence of $ZnF_2PMet@TiO_2$ and ROS scavengers: sodium azide (NaN_3) and sodium ascorbate (Asc).

degradation. The initially beneficial role of azide can be attributed to an enhanced generation of hydroxyl radicals stimulated by the presence of azide. Such effect was previously described by Hamblin *et al.*[49] The photocatalytic reaction is also affected by oxygen-centered radicals scavenger such as sodium ascorbate (Asc). A strong inhibition of the process by Asc and azide provides a convincing evidence for the participation of both of the reactive oxygen species: hydroxyl radicals and singlet oxygen. Their generation influences the photodegradation of the model organic pollutant (4-CP) and pharmaceutical (TRML).

Modest differences in the level of inhibition between the hydroxyl radical scavengers may be related to adsorption properties or slight differences in the experimental conditions. When singlet oxygen plays a significant role in the degradation processes the inhibition by azide is stronger than that observed for Asc, which inhibits the free radicals-mediated processes.

In the presence of Asc the relative reduction of oxygen consumption by azide is much smaller what also suggests that part of the oxygen is transformed into oxygen-centered radicals and the overall production is higher under heterogeneous than homogeneous conditions (photoreactions mediated by singlet oxygen).[35]

At both neat and modified TiO_2 generation of hydroxyl radicals takes place, as proven by electron paramagnetic resonance (EPR) measurements.[25,26] We have also published extensive ESR data that clarify the nature of the ROS produced by halogenated sulfonamide porphyrin and porphyrin derivatives.[4,37] However, in order to monitor hydroxyl radical generation in heterogeneous systems, we opted for the evaluation of the formation of hydroxyterephthalic acid (TAOH) in the reaction of terephthalic acid (TA) oxidation with hydroxyl radicals (Fig. 12). Terephthalic acid reacts rapidly with $HO^\bullet$ to produce hydroxyterephthalic acid, which is a highly fluorescent compound. The fluorescence intensity of TAOH is proportional to the amount of generated $HO^\bullet$ radicals.[50] Fig. 12 shows that the modification with ZnF_2PMet accelerates the TiO_2 photoactivity irradiated with visible light. $ZnF_2PMet@TiO_2$ is characterized by a higher efficacy of hydroxyl radical formation during visible light irradiation than bare, unmodified TiO_2 (P25).

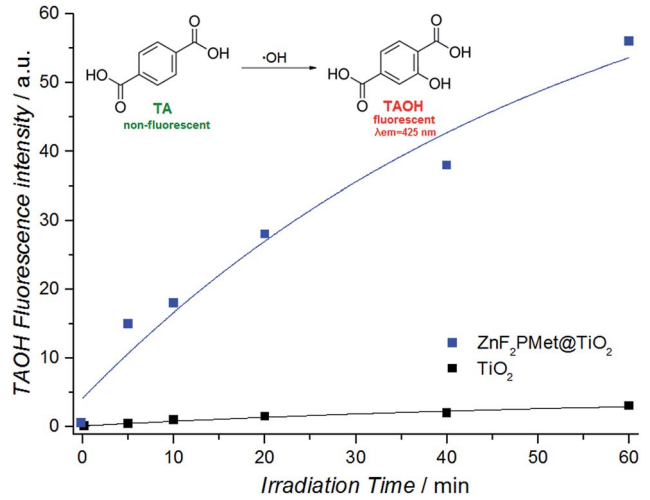

Fig. 12 Hydroxyl radicals generation in heterogeneous system: TAOH formation during irradiation of TiO_2 (P25) and $ZnF_2PMet@TiO_2$ suspended in TA solution (λ > 400 nm).

Hydroxyl radicals do not play a significant role in photodegradation of ZnF_2PMet in solution under our experimental conditions. However, photochemical tests with TA provide an evidence that hydroxyl radicals play an important role in $ZnF_2PMet@TiO_2$ photocatalytic degradation of TRML. Both mechanisms, electron transfer process (I type) and energy transfer with singlet oxygen generation (II type) are involved in the photodegradation of TRML with $ZnF_2PMet@TiO_2$ as a photocatalys, but the main pathway of TRML photodegradation in this heterogeneous system seems to be a Type I photoprocess. On the other hand, the major ROS generated in homogeneous system with ZnF_2PMet as a photosensitizer is singlet oxygen. This conclusion is confirmed by experiments with the singlet oxygen scavengers.

4. Conclusions

The metal complexes of 5,10,15,20-tetrakis(2,6-difluoro-5-*N*-methylsulfamylophenyl)porphyrin were prepared and characterized. The results of these studies show that some of these metal complexes can be considered as efficient photosensitizers for singlet oxygen generation and as photocatalysts for degradation of organic pollutants, both in solution and as a part of heterogeneous photocatalysts.

The zinc porphyrin derivative, ZnF_2PMet, is characterized by a high yield of singlet oxygen formation in solution ($\Phi_\Delta = 0.99$), and in this system the most reasonable mechanism of photocatalytic activation involves the energy transfer from the excited state of the photosensitizer (triplet state) to oxygen molecule. The significant photocurrent generation and the high photogeneration of hydroxyterephthalic acid from terephthalic acid in the illumination of $ZnF_2PMet@TiO_2$ with visible light, point at an additional role played by hydroxyl radicals in photocatalytic activity of $ZnF_2PMet@TiO_2$. The process of sensitization in hybrid materials may additionally involve the electron transfer from the dye to the conduction band of titanium dioxide. Examination of the photocatalytic activity of the composite materials on the pharmaceutical tramadol hydrochloride and a model organic pollutant (4-CP) with visible light showed a superior performance of $ZnF_2PMet@TiO_2$ over the standard TiO_2 (P25). The relatively good photostability and photoactivity of $ZnF_2PMet@TiO_2$ material may enable its practical applications, including not only photochemistry and photocatalysis but also photomedicine *e.g.* photodynamic therapy (PDT) or photoinactivation of microorganisms and bacterial cells.

Acknowledgements

This work was founded by the Ministry of Science and Higher Education, Poland, within the *Iuventus Plus* program, grant number 0085/IP3/2015/73 given to JMD. We also thank National Science Centre for the support (grant number 2012/05/BST5/00389). WM is indebted to the Ministry of Science and Higher Education for the support within the *Ideas Plus* project, grant No. IdP2012000362.

Notes and references

1 P. Joshi, T. O. Ahmadov, P. Wang and P. Zhang, *RSC Adv.*, 2015, **5**, 67892–67895.
2 J. M. Dąbrowski and L. G. Arnaut, *Photochem. Photobiol. Sci.*, 2015, **14**, 1765–1780.
3 J. M. Dąbrowski, L. G. Arnaut, M. M. Pereira, K. Urbańska, S. Simões, G. Stochel and L. Cortes, *Free Radical Biol. Med.*, 2012, **52**, 1188–1200.
4 (*a*) E. F. F. Silva, C. Serpa, J. M. Dąbrowski, C. J. P. Monteiro, S. J. Formosinho, G. Stochel, K. Urbanska, S. Simões, M. M. Pereira and L. G. Arnaut, *Chem.–Eur. J.*, 2010, **16**, 9273–9286; (*b*) J. M. Dąbrowski, K. Urbanska, L. G. Arnaut, M. M. Pereira, A. R. Abreu, S. Simões and G. Stochel, *ChemMedChem*, 2011, **6**, 465–475.
5 Y. Ge, X. Weng, T. Tian, F. Ding, R. Huang, L. Yuan, J. Wu, T. Wang, P. Guo and X. Zhou, *RSC Adv.*, 2013, **3**, 12839–12846.
6 (*a*) M. R. Hamblin and T. Hasan, *Photochem. Photobiol. Sci.*, 2004, **3**, 436–450; (*b*) Y. Fang, T. Liu, Q. Zou, Y. Zhao and F. Wu, *RSC Adv.*, 2015, **5**, 56067–56074.
7 M. Tarr and D. P. Valenzo, *Photochem. Photobiol. Sci.*, 2003, **2**, 355–361.
8 A. Jańczyk, E. Krakowska, G. Stochel and W. Macyk, *J. Am. Chem. Soc.*, 2006, **128**, 15574–15575.
9 G. Lente and J. H. Espenson, *Chem. Commun.*, 2003, 1162–1163.
10 J. Mosinger and Z. Micka, *J. Photochem. Photobiol., A*, 1997, **107**, 77–82.
11 A. V. C. Simoes, A. Adamowicz, J. M. Dąbrowski, M. J. F. Calvete, A. R. Abreu, G. Stochel, L. G. Arnaut and M. M. Pereira, *Tetrahedron*, 2012, **68**, 8767–8772.
12 J. M. Dąbrowski, M. M. Pereira, L. G. Arnaut, C. J. P. Monteiro, A. F. Peixoto, A. Karocki, K. Urbanska and G. Stochel, *Photochem. Photobiol.*, 2007, **83**, 897–903.
13 L. G. Arnaut and S. J. Formosinho, *Pure Appl. Chem.*, 2013, **85**, 1389–1403.

14 K. M. Kadish, K. M. Smith and R. Guilard, *The porphyrin handbook*, Academic Press, San Diego, 2000.
15 C. Serpa, J. Schabauer, A. P. Piedade, C. J. P. Monteiro, M. M. Pereira, P. Douglas, H. D. Burrows and L. G. Arnaut, *J. Am. Chem. Soc.*, 2008, **130**, 8876–8877.
16 D. Wróbel and A. Dudkowiak, *Mol. Cryst. Liq. Cryst.*, 2006, **448**, 15–38.
17 M. Ethirajan, Y. Chen, P. Joshi and R. K. Pandey, *Chem. Soc. Rev.*, 2010, **40**, 340–362.
18 M. M. Pereira, C. J. P. Monteiro, A. V. C. Simões, S. M. A. Pinto, A. R. Abreu, G. F. F. Sá, E. F. F. Silva, L. B. Rocha, J. M. Dąbrowski, S. J. Formosinho, S. Simões and L. G. Arnaut, *Tetrahedron*, 2010, **66**, 9545–9551.
19 (*a*) M. Silva, M. E. Azenha, M. M. Pereira, H. D. Burrows, M. Sarakha, M. F. Ribeiro, A. Fernandes, P. Monsanto and F. Castanheira, *Pure Appl. Chem.*, 2009, **81**, 2025–2033; (*b*) M. Silva, M. E. Azenha, M. M. Pereira, H. D. Burrows, M. Sarakha, C. Forano, M. F. Ribeiro and A. Fernandes, *Appl. Catal., B*, 2010, **100**, 1–9.
20 K. Szaciłowski, W. Macyk, A. Drzewiecka-Matuszek, M. Brindell and G. Stochel, *Chem. Rev.*, 2005, **105**, 2647–2694.
21 S. Faulkner and J. Matthews, in *Comprehensive Coordination Chemistry II*, ed. J. A. McCleverty and T. J. Meyer, Elsevier, Amsterdam, 2003.
22 H. D. Burrows, M. L. Canle, J. A. Santaballa and S. Steenken, *J. Photochem. Photobiol., B*, 2002, **67**, 71–108.
23 M. Bellardita, V. Loddo, A. Mele, W. Panzeri, F. Parrino, I. Pibiri and L. Palmisano, *RSC Adv.*, 2014, **4**, 40859–40864.
24 O. Legrini, E. Oliveros and A. M. Braun, *Chem. Rev.*, 1993, **93**, 671–698.
25 S. Liu, Z.-R. Tang, Y. Sun, J. C. Colmenares and Y.-J. Xu, *Chem. Soc. Rev.*, 2015, **44**, 5053–5075.
26 N. Zhang, M.-Q. Yang, S. Liu, Y. Sun and Y.-J. Xu, *Chem. Rev.*, 2015, **115**, 10307–10377.
27 B. Weng, S. Liu, Z.-R. Tang and Y.-J. Xu, *RSC Adv.*, 2014, **4**, 12685–12700.
28 H. Gnaser, M. R. Savina, W. F. Calaway, C. E. Tripa, I. V. Veryovkin and M. J. Pellin, *Int. J. Mass Spectrom.*, 2005, **245**, 61–67.
29 M. Bergheim, R. Giere and K. Kummerer, *Environ. Sci. Pollut. Res.*, 2012, **19**, 72–85.
30 P. C. Rua-Gomez and W. Puttmann, *Chemosphere*, 2013, **90**, 1952–1959.
31 (*a*) E. Silva, M. M. Pereira, H. D. Burrows, M. E. Azenha, M. Sarakha and M. Bolte, *Photochem. Photobiol. Sci.*, 2004, **3**, 200–204; (*b*) S. L. H. Rebelo, A. Melo, R. Coimbra, M. E. Azenha, M. M. Pereira, H. D. Burrows and M. Sarakha, *Environ. Chem. Lett.*, 2007, **5**, 29–33; (*c*) C. J. P. Monteiro, M. M. Pereira, M. E. Azenha, H. D. Burrows, C. Serpa, L. G. Arnaut, M. J. Tapia, M. Sarakha, P. Wong-Wah-Chung and S. Navaratnam, *Photochem. Photobiol. Sci.*, 2005, **4**, 617–624.
32 (*a*) J. M. Dąbrowski, M. Krzykawska, L. G. Arnaut, M. M. Pereira, C. J. P. Monteiro, S. Simões, K. Urbanska and G. Stochel, *ChemMedChem*, 2011, **6**, 1715–1726; (*b*) J. M. Dąbrowski, L. G. Arnaut, M. M. Pereira, C. J. P. Monteiro, K. Urbanska, S. Simões and G. Stochel, *ChemMedChem*, 2010, **5**, 1770–1780.
33 (*a*) J. M. Dąbrowski, L. G. Arnaut, M. M. Pereira, K. Urbanska and G. Stochel, *MedChemComm*, 2012, **3**, 502–505; (*b*) R. Saavedra, L. B. Rocha, J. M. Dąbrowski and L. G. Arnaut, *ChemMedChem*, 2014, **9**, 390–398; (*c*) M. Krzykawska-Serda, J. M. Dąbrowski, L. G. Arnaut, M. Szczygiel, K. Urbanska, G. Stochel and M. Elas, *Free Radical Biol. Med.*, 2014, **73**, 239–251; (*d*) L. B. Rocha, L. Gomes-da-Silva, J. M. Dąbrowski and L. G. Arnaut, *Eur. J. Cancer*, 2015, **51**, 1822–1830.
34 J. M. Dąbrowski, B. Pucelik, M. M. Pereira, L. G. Arnaut and G. Stochel, *J. Coord. Chem.*, 2015, **68**, 3116–3134.
35 B. Yaoa, C. Penga, W. Zhang, Q. Zhanga, J. Niua and J. Zhaoa, *Appl. Catal., B*, 2015, **174–175**, 77–84.
36 H. Ghafuri, Z. Movahedinia, R. Rahimi and H. Zand, *RSC Adv.*, 2015, **5**, 60172–60178.
37 L. G. Arnaut, M. M. Pereira, J. M. Dąbrowski, E. F. F. Silva, F. A. Schaberle, A. A. Abreu, L. B. Rocha, M. M. Barsam, K. Urbanska, G. Stochel and C. M. A. Brett, *Chem.–Eur. J.*, 2014, **20**, 5346–5357.
38 E. F. F. Silva, F. A. Schaberle, C. J. P. Monteiro, J. M. Dąbrowski and L. G. Arnaut, *Photochem. Photobiol. Sci.*, 2013, **12**, 1187–1192.
39 M. Strlič, J. Kolar, V.-S. Šelih, D. Kočar and B. Pihlar, *Acta Chim. Slov.*, 2003, **50**, 619–632.
40 S. Leonard, P. M. Gannett, Y. Rojanasakul, D. Schwegler-Berry, V. Castranova, V. Vallyathan and X. Shi, *J. Inorg. Biochem.*, 1998, **70**, 239–244.
41 G. Mele, R. del Sole, G. Vasapollo, E. Garcia-Lopez, L. Palmisano, L. Jun, R. Słota and G. Dyrda, *Res. Chem. Intermed.*, 2007, **33**, 433–448.
42 Z. Tachan, I. Hod and A. Zaban, *Adv. Energy Mater.*, 2014, **4**, 1301249.
43 M. Buchalska, P. Łabuz, Ł. Bujak, G. Szewczyk, T. Sarna, S. Maćkowski and W. Macyk, *Dalton Trans.*, 2013, **42**, 9468–9475.
44 D. V. Heyd and B. Au, *J. Photochem. Photobiol., A*, 2005, **174**, 62–70.
45 X.-T. Zhou, H.-B. Ji and X.-J. Huang, *Molecules*, 2012, **17**, 1149–1158.
46 X. Lu, N. Hu, J. Li, H. Ma, K. Du and R. Zhao, *Res. Chem. Intermed.*, 2014, **40**, 1911–1922.
47 S. Murphy, C. Saurel, A. Morrissey, J. Tobin, M. Oelgemoller and K. Nolan, *Appl. Catal., B*, 2012, **15**, 119–120.
48 S. Sardar, P. Kar and S. K. Pal, *Journal of Materials NanoScience*, 2014, **1**, 12–30.
49 L. Huang, T. G. St Denis, Y. Xuan, Y. Y. Huang, M. Tanaka, A. Zadlo, T. Sarna and M. R. Hamblin, *Free Radical Biol. Med.*, 2012, **53**, 2062–2071.
50 T. Hirakawa and Y. Nosaka, *Langmuir*, 2002, **18**, 3247–3254.